THE BELL SYSTEM TECHNICAL JOURNAL
Vol. 58, No. 5, May–June 1979
Printed in U.S.A.

Digital Radio Outage Due to Selective Fading—Observation vs Prediction From Laboratory Simulation

By C. W. LUNDGREN and W. D. RUMMLER

(Manuscript received July 7, 1978)

A statistical model (introduced in a companion paper) of fading on a radio path is used with laboratory measurements on a digital radio system to estimate the outage due to multipath fading, where outage is the time that the bit error rate (BER) exceeds a threshold. Over the range of BER of interest (10^{-6} to 10^{-3}), the calculated outage agrees favorably with the outage observed during the period for which the fading model was developed. It is further shown that the calculated outage, when scaled to a heavy fading month on the basis of single-frequency, time-faded statistics, agrees equally well with the outage observed on the same path during a heavy fading month. The agreement between measured and predicted outage substantiates the selective fading model. The prescribed laboratory measurements characterize the sensitivity of the radio system to selective fading. Thus, the methodology provides a useful basis for comparing the outage of alternative realizations of digital radio systems.

I. INTRODUCTION

Present interest in using high-speed common carrier digital radio[1–5] has precipitated a need for estimating the performance of such systems during periods of selective (multipath) fading. This paper describes a method of characterizing a digital radio system in the laboratory which allows the outage to be accurately estimated. For a digital radio system, outage requirements are stated in terms of the number of seconds in a time period (usually a heavy fading month) during which the bit error rate (BER) may exceed a specified level; typically, 10^{-3} or 10^{-4} is appropriate to voice circuit application.

The method is based upon a statistical channel model[6] developed from measurements on an unprotected 26.4-mile hop in the 6-GHz band in Palmetto, Georgia in 1977 using a general trade 8-PSK digital

radio system as a channel measuring probe. The modeled fading occurrences were scaled to the basis of a heavy fading month using the occurrence of time faded below a level at a single frequency as the means of calibration. The bit error rate performance of the digital radio system was measured during the time period used for channel modeling and for an extended period corresponding to a heavy fading month. This same radio system was later subjected to a measurement program in the laboratory using a multipath simulator which provides a circuit realization of the fading model. The measured results are used with the channel model to determine the occurrence of channel conditions which will cause the BER to exceed a given threshold. Comparisons on the basis of the modeling period and a heavy fading month show good agreement between calculated and observed outages for BERs between 10^{-6} and 10^{-3}.

The properties of the fixed-delay channel model are reviewed briefly in Section II as a basis for describing the measurements and for the subsequent outage calculations. This three-parameter channel model is realized in the laboratory by an IF fade simulator. The simulator and its use in obtaining the necessary laboratory data are described in Section III. The procedures to be followed in calculating outage times for a given BER are described in Section IV. Calculated and observed outage times are compared in Section V. Conclusions are provided in Section VI.

II. MODEL DESCRIPTION—METHODOLOGY

It has been demonstrated[6] that the complex voltage transfer function of a line-of-sight microwave radio channel is well modeled by the function

$$H(\omega) = a\,[1 - be^{-j(\omega-\omega_0)\tau}] \tag{1}$$

with τ fixed. A 6-GHz channel (30-MHz bandwidth) has been characterized statistically by the model with $\tau = 6.3$ ns. Such a channel has a power transfer function given by

$$|H(\omega)|^2 = a^2[1 + b^2 - 2b\cos(\omega - \omega_0)\tau] \tag{2}$$

and an envelope delay distortion function, i.e., the derivative of the phase of $H(\omega)$ with respect to ω, given by

$$D(\omega) = \frac{b\tau(\cos(\omega - \omega_0)\tau - b)}{1 + b^2 - 2b\cos(\omega - \omega_0)\tau}. \tag{3}$$

In the following paragraphs, we summarize the properties of the model, the statistics of the model parameters, and the measurement objectives.

2.1 Fixed delay model

A plot of the attenuation produced by the fixed delay model of eq. (1) is shown in Fig. 1. Since the delay is fixed at 6.3 ns, the spacing between nulls of the response, 158.4 MHz, is much larger than the channel bandwidth. The parameters a and b control the depth and shape of the simulated fade, respectively. The parameter $f_o(=\omega_0/2\pi)$ determines the position of the fade minimum or notch. Both the notch frequency, f_o, and the response frequency, f, are measured from the center of the 30-MHz channel for convenience.

The model function of eq. (1) may be interpreted as the response of a channel which provides a direct transmission path with amplitude a and a second path providing a relative amplitude b at a delay of 6.3 ns and with a phase of $\omega_0\tau + \pi$ (independently controllable) at the center frequency of the channel. This interpretation is represented in Fig. 2 by a phasor diagram at $\omega = 0$, the center frequency of the channel. Varying the frequency, ω, over the channel bandwidth (30 MHz) moves the angle of the interfering ray through an arc of about 60 degrees ($2\pi \times 30$ MHz $\times$ 6.3 ns $\approx \pi/3$), centered at the position shown. This diagram is useful for understanding the fade simulation; it also provides an alternate means of describing the position of the notch. The notch position may be specified by its frequency, f_o, or by ϕ, the angle of the interfering path at the center of the channel.

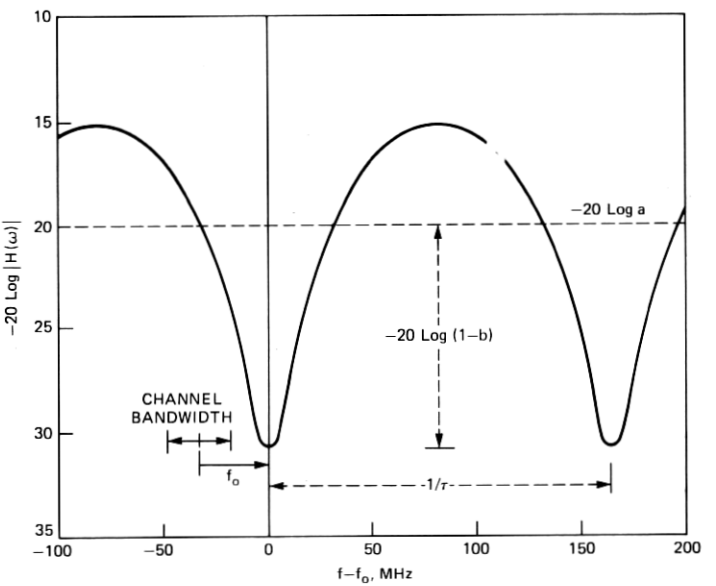

Fig. 1—Attenuation of channel model function, $H(\omega) = a[1 - b\exp(-j(\omega - \omega_0)\tau)]$, for $\tau = 6.3$ ns, $a = 0.1$, $b = 0.7$.

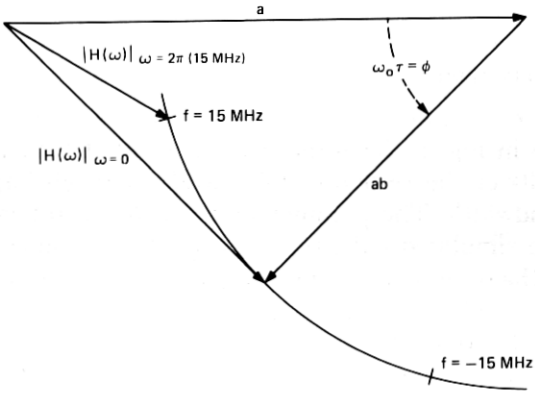

Fig. 2—Phasor diagram of a modeled fade, $\phi = 45°$, $b = 0.7$.

From Figs. 1 and 2, or eq. (1), it may be seen that varying a changes the overall level and varying b changes the shapeliness of the modeled fade. Furthermore, if the minimum is within the 30-MHz channel bandwidth ($|\phi| < 30°$), the fixed delay model can generate notches with a wide range of levels and notch widths. With the minimum out of band, it can generate a wide range of combinations of levels, slopes, and curvatures within the channel bandwidth.

2.2 Model statistics

The statistics of the model parameters were obtained from a selected data base during which heavy fading activity was observed.[6] The distribution of b is best described in terms of $B = -20 \log(1 - b)$. Figure 3 shows the distribution of B and the least-squares straight line fit to the distribution over the region where it best represents selective fading—between B values of 3 and 23 dB. The channel is described by B greater than 23 dB for less than 0.15 percent of the observed time which makes the distribution less certain beyond this point. At the other extreme, during the periods of time when there is little or no selective fading, the channel is characterized by values of B less than 3 dB. Thus, the fitted line represents a lower bound on the distribution for B less than 3 dB. Since the fitted line has an intercept of 5400 seconds, we may model the fraction of 5400 seconds during which B exceeded a value X by the probability distribution

$$P(B > X) = e^{-X/3.8}. \tag{4}$$

Thus the probability of finding a value of B between X and $X + dX$ is

$$p_B(X)\, dX = \frac{dX}{3.8}\, e^{-X/3.8}. \tag{5}$$

The distribution of a is lognormal with a standard deviation of 5 dB and a mean that is dependent on B (or b). Hence, the probability that

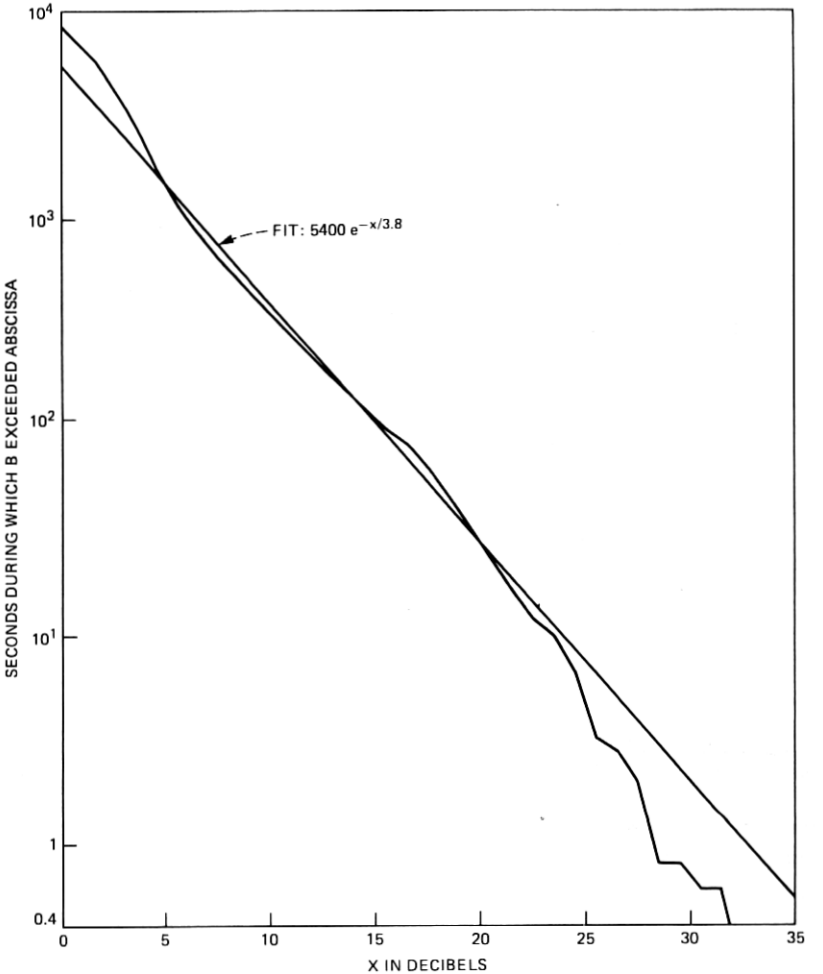

Fig. 3—Distribution of B for model data base period.

$A = -20 \log a$ has a value between Y and $Y + dY$ is given by

$$p_A(Y)\, dY = \frac{dY}{5\sqrt{2\pi}}\, e^{-[Y - A_0(B)]^2/50}. \tag{6}$$

The relationship between A_0, the mean of the distribution, and B is given in Fig. 4.

The distribution of f_o is found to be independent of A and B. It is usually simpler to work with ϕ rather than f_o. The two variables are simply related in that ϕ is defined on the interval $(-\pi, \pi)$ and a 2.5-degree change in ϕ corresponds to a 1.1-MHz change in f_o. For the fixed delay model, the variable ϕ has been found to have a probability density function that can be described as uniform at two levels, with

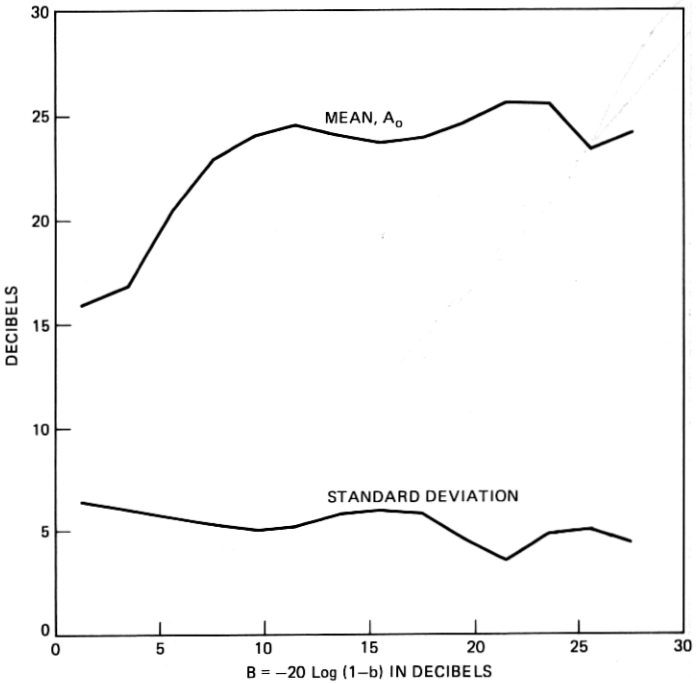

Fig. 4—Mean and standard deviation of the distribution of $A = -20 \log a$ as a function of B.

values less than $\pi/2$ being five times more likely than values greater than $\pi/2$. Thus, we have the probability density function per degree as:

$$p_\phi(\phi) = \begin{cases} \dfrac{1}{216} & |\phi| < 90° \\ \dfrac{1}{1080} & 90° \leq |\phi| \leq 180. \end{cases} \tag{7}$$

The functions in eqs. (5) to (7) can be used to determine the probability of finding a, b, and f_o in some region of a-b-f_o space. This probability can be converted to number of seconds in the observation period by multiplying by 5400 seconds. To convert this probability to the number of seconds in a month requires scaling the data base. The scaling may be obtained from Fig. 5 which shows, for several frequencies in the band, the time during the model data base period that the channel was faded below a given level. Distributions are shown for average power in the band and for power at selected frequencies at the center and near the edges of the radio channel. (Frequencies indicated are at IF where the center frequency is at 70 MHz.) For the path used,

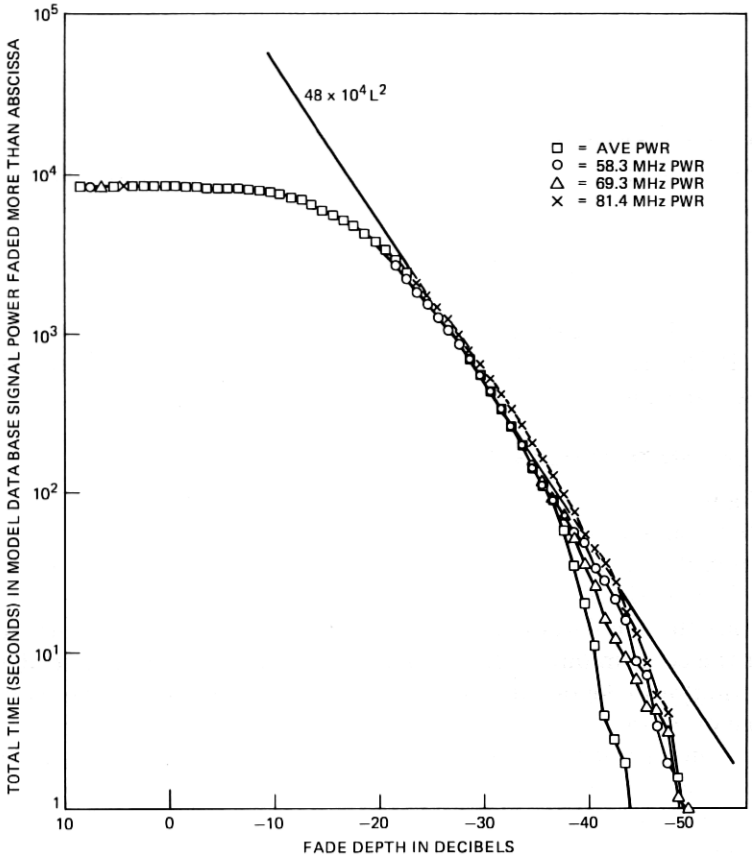

Fig. 5—Amplitude distributions for model data base period.

one expects the received voltage (single frequency) relative to midday average to be less than L for $72.5 \times 10^4 L^2$ seconds in a month.[7] For the data base used, the fading is best described by $48 \times 10^4 L^2$ hence, the data represent ⅔ of a fading month. To obtain outage on a seconds-per-heavy-fading-month basis, the probabilities calculated with eqs. (5) to (7) must be multiplied by 5400×1.5 or 8100 seconds.

2.3 Outage estimation

The fixed delay model described above can be simulated with an equivalent circuit laboratory measurement to determine the equipment response to multipath fading. Conceptually, one determines critical values of A and B for which a specified error rate is achieved for each fade notch position. In practice, it is difficult to maintain a constant BER; it is more expedient to fix b and vary the carrier-to-noise ratio (a) while plotting the BER. From the resulting curves, one may

compute critical contours of A and B for each prescribed notch location and BER. Using eqs. (5) and (6), the probability that A and B lie on the high error rate side of a given critical contour may be calculated.

By repeating this calculation for a uniform set of notch positions and using (7) to determine the probability weighting given to each and summing, one may estimate the probability of all selective fades that produce a BER exceeding the prescribed one. Multiplying this probability by 5400 gives the outage time expected over the data base period; multiplying by 8100 gives the expected outage time per heavy fading month.

The following section describes the laboratory measurement; Section IV describes the reduction of the measured curves and parameters to outage times.

III. LABORATORY MEASUREMENTS

Figure 6 illustrates stressing of a digital radio system by means of an IF fade simulator. The simulator, which is inserted after linear IF preamplification but before any high-gain amplification, shapes both the desired signal and the effective received noise. It is necessary to operate the simulator at a sufficiently large input carrier-to-noise ratio that the concomitantly shaped noise at its output remains a negligible contributor to degraded system performance throughout the operating range of interest.

Within its restricted frequency range of operation, the IF simulator is adjusted to achieve those specific shapes implied by Fig. 2. Although the measurements could have been made using an RF fade simulator, the choice of an IF simulator was based primarily upon considerations of signal and noise levels, and the repeatability of adjustments. The following section describes an IF shape-stressing measurement in the minimum detail necessary to qualify the data collected.

3.1 Representative IF two-path fade stressing measurement

The block diagram of Fig. 7 illustrates an arrangement employing an IF fade simulator and an IF flat noise source. A pseudo-random test

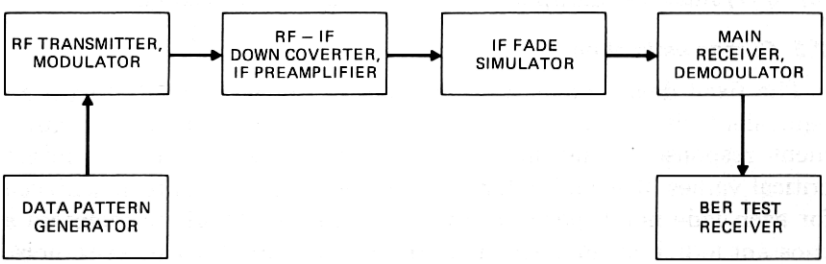

Fig. 6—IF fade stressing.

pattern modulates the 6-GHz radio transmitter whose output is nominally 5 watts (ⓐ, in Fig. 7). The output spectrum is usually shaped by a bandpass filter following the microwave power amplifier to comply with FCC regulations.

To enable back-to-back operation of the transmitter and receiver of a single repeater which normally operate on different radio channels, a radio test translator was employed. The translator output power was approximately −30 dBm (adjustable, at ⓑ) to simulate the unfaded received signal level (RSL) observed typically in the field.

Assuming a linear RF-IF conversion gain of 20 dB, the signal power at the input (ⓒ) to the IF fade simulator is −10 dBm. The simulator incorporates low-noise linear amplification. A reference insertion loss for the main unfaded ray is 10 dB, including the output power summer. Hence the maximum desired signal power at the input to the main IF amplifier (ⓔ) is −20 dBm.

Assuming a 30-MHz receiver noise bandwidth and a current-art receiving system noise figure of 5 dB, the total system noise power is approximately −95 dBm, referred to the receiver's input port. This results in a flat receiver noise contribution of −85 dBm at input ⓔ to the main IF amplifier. Consequently, the maximum attainable carrier to simulator-shaped RF noise ratio is 10 log $(C_0/N_{rf}) = -20 - (-85) =$ 65 dB. The noise contributed by the fade simulator amplifiers must not exceed −100 dBm, to be negligible.

Flat IF noise much larger than the unwanted and shaped system noise is added artificially at ⓔ and is adjusted in magnitude by a calibrated attenuator ⓓ to superpose thermal noise degradations upon the simulated selective fading degradations of the desired signal. One would ideally measure the added IF noise power in the final predetection bandwidth of the digital radio system, or twice the Nyquist bandwidth. It is more convenient in the laboratory to reference carrier-to-noise ratios to the output of the main IF amplifier by using the precalibrated AGC voltage (assuming that wideband AGC detection is employed), to measure both the unshaped signal and noise powers. The carrier-to-noise ratio at the detector would be higher—by the ratio of the system noise bandwidths that would be measured at the respective points.

The noise source output in Fig. 7 may be adjusted so that an attenuator setting of 0 dB ⓓ results in a noise power equivalent to that of the unfaded signal power (the attenuator is then calibrated directly in uncorrected C_0/N_{if}, in dB). As the IF fade simulator is readjusted to achieve different prescribed fade shapes, its mean insertion loss may also change. The change in insertion loss is determined by monitoring the change in signal power at ⓔ; the same loss increment (dB) must be added to the noise attenuator ⓓ to reestablish the 0 dB reference.

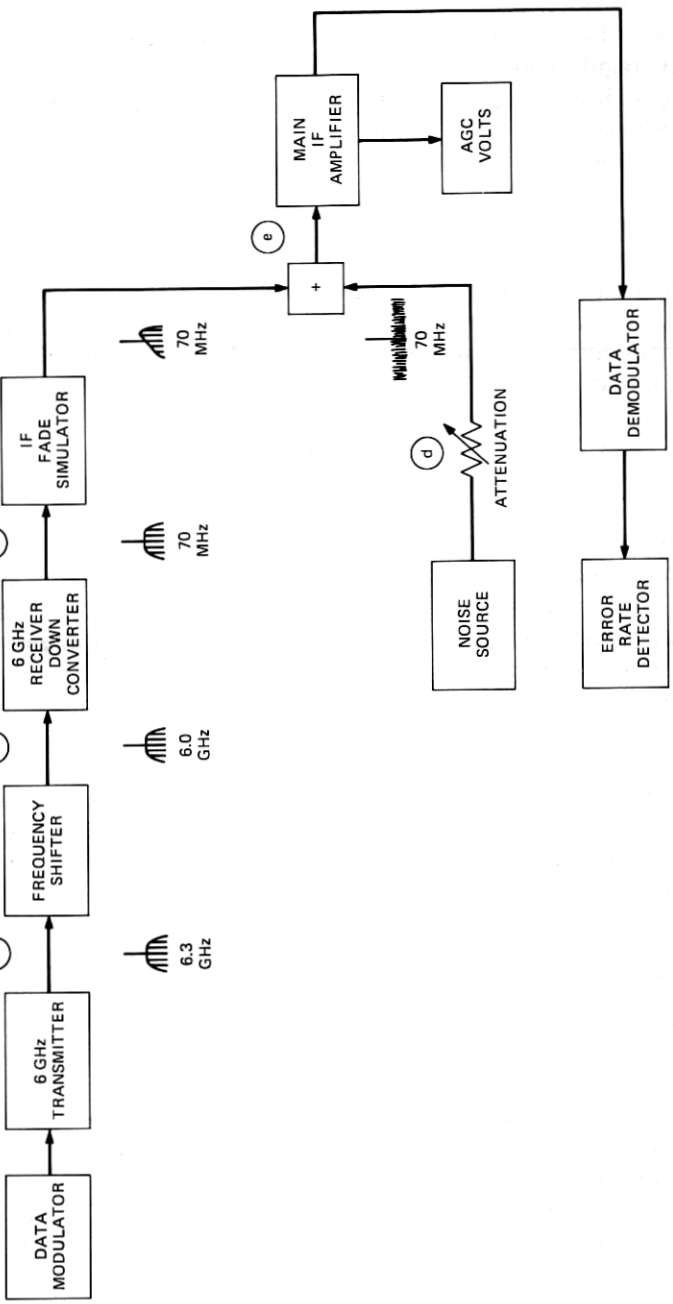

Fig. 7—Laboratory test arrangement.

3.2 IF two-path fade simulator

Figure 8 illustrates splitting the desired IF signal into an arbitrarily phased, adjustable "main" component and a "delayed" component fixed in delay (τ ns) but adjustable in magnitude. The main component is further resolved into orthogonal components (inset to Fig. 8) using wideband networks exhibiting flat gain and well-behaved delay. A particular sum vector is constructed by adjusting the orthogonal components to establish a simulated fade notch frequency; in practice, the phase sense of 0- and 90-degree components are independently reversible, as indicated by the switches in the figure, for complete flexibility in notch frequency selection.

The 6.3-ns fixed delay added to the delayed path imparts a phase shift of 159 degrees at the 70-MHz IF center frequency. This is shown built out to 225 degrees, relative to the 0-degree transmission path, using a 66-degree wideband network of the same type. The delayed vector is fixed in direction opposite the midrange position of the adjustable main vector, corresponding to a channel-centered fade (ϕ = 0 degrees).

Since $1/\tau = 158.4$ MHz, a change of 1 degree in direction of the main vector corresponds to a frequency displacement of the fade notch location of 0.44 MHz. For $\phi = -45$ degrees, the notch location is displaced 19.8 MHz below the channel center ($f_o = -19.8$ MHz). The magnitude of the delayed component is then adjusted to achieve the desired notch depth.

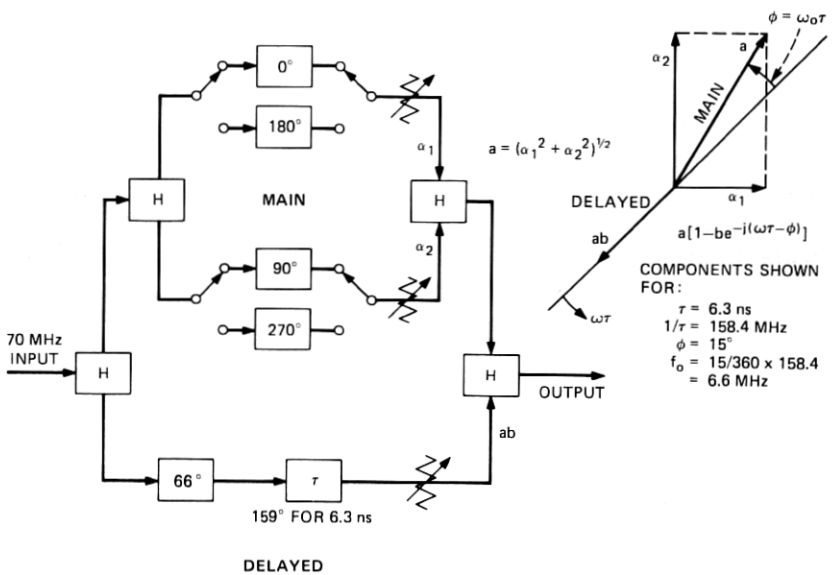

Fig. 8—IF fade simulator—conceptual block diagram.

3.3 Digital radio performance stressed by in-band selectivity and thermal noise

The radio equipment was measured at uniformly spaced notch frequencies separated by 4.4 MHz ($\Delta\phi = 10$ degrees). To fully characterize a period of variation in ϕ, or f_o, one would need to make 36 sets of measurements. *Ideally,* half may be omitted because of symmetry. For given values of A and B, the same error rate should obtain for a notch at a given frequency displacement above or below the channel band center. Variations in B ought not to have a significant effect for $|\phi|$ greater than 90 degrees. It was determined that detailed measurements were required for nine different values of f_o to characterize the digital radio tested.

Using a wideband RF fade simulator in the field, the digital radio performance for out-of-channel notch locations was relatively independent of whether minimum or nonminimum-phase fade simulations were employed. The nonminimum phase fade is modeled by eq. (1) with the sign of the phase term reversed. This leaves the amplitude [eq. (2)] unchanged, but reverses the sign of the envelope delay distortion [eq. (3)]. We conclude that the minimum phase channel model is sufficiently general for use in simulating the channel and in estimating performance.

The IF fade simulator was adjusted for each notch frequency, and the depth of notch was varied by adjusting the magnitude of the delayed component. Then various amounts of IF thermal noise were added. Figure 9 typifies the performance data collected. BERs are plotted *versus* the uncorrected IF carrier-to-noise ratio (C/N_{if}), for a constant fade notch offset from midchannel ($f_o = -19.8$ MHz, $\tau = 6.3$ ns). Each curve corresponds to a different notch depth ($B = -20 \log(1-b)$ dB), and hence a different amplitude and delay shape in the radio channel. Each curve is also identified with an in-band selectivity, defined as the difference between the maximum and minimum attenuation present in the (25.3-MHz) channel bandwidth. The lower-left "baseline" curve presents the unshaped signal, flat fading performance obtained by adding only IF thermal noise. This curve was verified (without the added IF noise) by attenuating the received RF input signal in the back-to-back configuration.

Consideration was given to matching the order of measurements to characteristics of the particular digital radio tested. For example, considerable scattering of data at low error rates can result from synchronizations involving different reference carrier phases. The authors elected to perform several synchronizations while observing the BER for each phase, and then chose that phase giving the worst performance.* Synchronization was accomplished at the low error rate

* Because the phase information in the measured system was Gray coded and digital access was on a per-rail basis, one rail had twice the BER of the other two. All measurements in the field and in the laboratory were made on this worst-case rail.

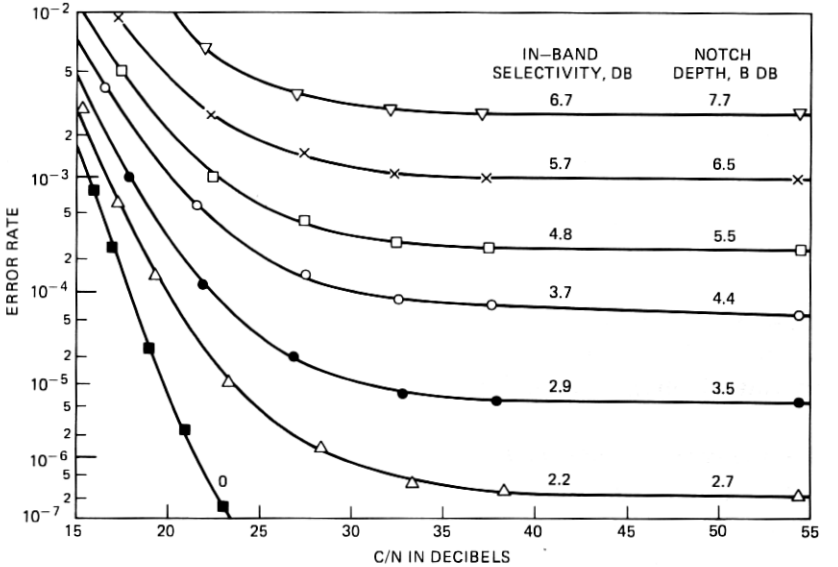

Fig. 9—High-speed digital radio IF dispersive fade simulations, $\tau = 6.3$ *ns*, $f_0 = -19.8$ MHz.

(bottom) of each curve, and this phase relationship was maintained for all data points obtained for each curve.

From the baseline curve of Fig. 9, a BER $= 1 \times 10^{-6}$ obtains for 10 $\log(C/N_{if}) \doteq 21.5$ dB. For the digital radio system installed on the instrumented hop and reported in the figure, the measured flat fade margin for a threshold BER $= 1 \times 10^{-6}$ was 40.5 dB This leads to an unfaded IF carrier-to-noise ratio 10 $\log(C_0/N_{if}) \doteq 21.5 + 40.5 = 62$ dB.

From the baseline curve for a BER $= 1 \times 10^{-7}$, note that insertion of a fade whose notch depth is 6.5 dB results in four orders of magnitude degradation in BER performance; equivalently, an in-band selectivity of only 5.7 dB in 25.3 MHz results in a BER $> 1 \times 10^{-3}$.

The asymptotic regions in Fig. 9, corresponding to high values of C/N_{if}, are not normally presented in characterizations of this type; however, system outage depends primarily upon the performance in these asymptotic regions. Thus, under typical fading conditions, the transmitted carrier power might be increased at will without improving the BER significantly. The effects of decreasing the carrier power are discussed in Section 4.4.

A family of curves like those shown in Fig. 9 was obtained (but are not given here) for each of nine uniformly spaced frequency offsets below midchannel to characterize the digital radio system sufficiently for the prediction of outage. A number of spot checks were also made using both RF and IF fade simulators at symmetrical positive and negative offset frequencies, to establish that acceptable symmetry existed.

IV. CALCULATION OF OUTAGE

This section describes four methods of calculating outage. The derivation of the critical curves of A and B, which provide the basis for making and understanding these calculations, is given in Section 4.1. In Section 4.2 the detailed calculation of outage from the critical A-B curves is described. It is shown in Section 4.3 that for the present system this method may be greatly simplified by calculating only selectivity-caused outage (i.e., neglecting thermal noise). Section 4.4 presents an approximate method of accounting for the effects of thermal noise. Section 4.5 provides a basis for estimating the selectivity-caused outage from a single measurement.

4.1 Derivation of critical characteristics

To calculate the outage for a fixed bit error rate, one must first obtain the critical curves of A and B at each simulated value of f_o, the notch position. Thus, from Fig. 9 which corresponds to $f_o = -19.8$ MHz (or $\phi = -45°$), we obtain six points on the critical curve of A and B for a BER of 10^{-3}, one point from each of the six curves which cross the critical BER. The value of B is obtained from the value of b since

$$B = -20 \log(1 - b). \tag{8}$$

For the curve in Fig. 9 corresponding to $B = 4.4$ dB, we obtain the corresponding critical value of A for a BER of 10^{-3} from the value of carrier-to-noise ratio, which is 20.2 dB where this curve crosses the 10^{-3} BER line. Since the carrier-to-noise ratio is 62 dB when the channel is unfaded, the 20.2 dB value corresponds to a relative average power loss of 41.8 dB,

$$L_s = 62 - 20.2 = 41.8 \text{ dB}. \tag{9}$$

Without loss of generality, we assume that the PSK signal has a rectangular spectrum of width f_b; consequently, the relative power transmitted by the model is obtained from eq. (2) as*

$$P_{av} = \frac{1}{2\pi f_b} \int_{-\pi f_b}^{\pi f_b} |H(\omega)|^2 \, d\omega$$

$$= a^2 \left\{ 1 + b^2 - 2b \cos 2\pi f_o \tau \left(\frac{\sin \pi f_b \tau}{\pi f_b \tau} \right) \right\}. \tag{10}$$

* The calculated result is not critically dependent on the flatness of the signal spectrum or the spectral width chosen. We have used for f_b a value of 25.3 MHz as representing the effective width of the signal.

Defining a correction term by

$$C = -10 \log\left\{1 + b^2 - 2b \cos 2\pi f_o \tau \left(\frac{\sin \pi f_b \tau}{\pi f_b \tau}\right)\right\}, \tag{11}$$

we may express the signal loss as

$$L_s = -10 \log P_{av} = A + C. \tag{12}$$

Thus, we obtain the critical value of A as

$$A = L_s - C. \tag{13}$$

For $B = 4.4$ dB ($b = 0.4$) and $f_o = -19.8$ MHz, we find $C = 2.06$ dB and the critical value of A is $41.8 - 2.1 = 39.7$ dB.

Carrying out these calculations for the six curves in Fig. 9, one can generate the critical curve of A and B for $f_o = -19.8$ MHz and a BER of 10^{-3}. The curve is shown in Fig. 10 along with the critical curves for several other values of the BER. A complete set of curves must be generated for all values of f_o.

The curves in Fig. 10 are typical of the critical curves obtained for $|f_o| \leq 33$ MHz. The intercept with the A-axis represents the flat fade margin for the given BER; this margin is independent of notch position. The intercept of a critical contour with the B-axis represents the shape, or relative fade depth, margin for the given notch position. For values of B to the right of this intercept, the critical value of BER cannot be obtained at any carrier-to-noise ratio for the given notch position.

4.2 Outage calculation— detailed method

The probability, P_o, of finding A and B outside all critical contours may be written with eqs. (5), (6), and (7) as

$$P_o = \int_{-\pi}^{\pi} p_\phi(\phi) P_c(\phi)\, d\phi, \tag{14}$$

where

$$P_c(\phi) = \int_0^\infty \int_{A_c(X)}^\infty p_A(Y) p_B(X)\, dY\, dX, \tag{15}$$

and $A_c(X)$ is the functional relation of the critical values of A to B (or X), for B less than B_c, the B-axis intercept, and for a given BER and ϕ value.* Since measurements were made for a uniformly spaced set of notch positions with spacing $\Delta\phi = 10°$, we may approximate (14) by

* The dependence of the function $A_c(X)$ and the asymptote B_c on BER and ϕ is not explicitly denoted to keep notation simple.

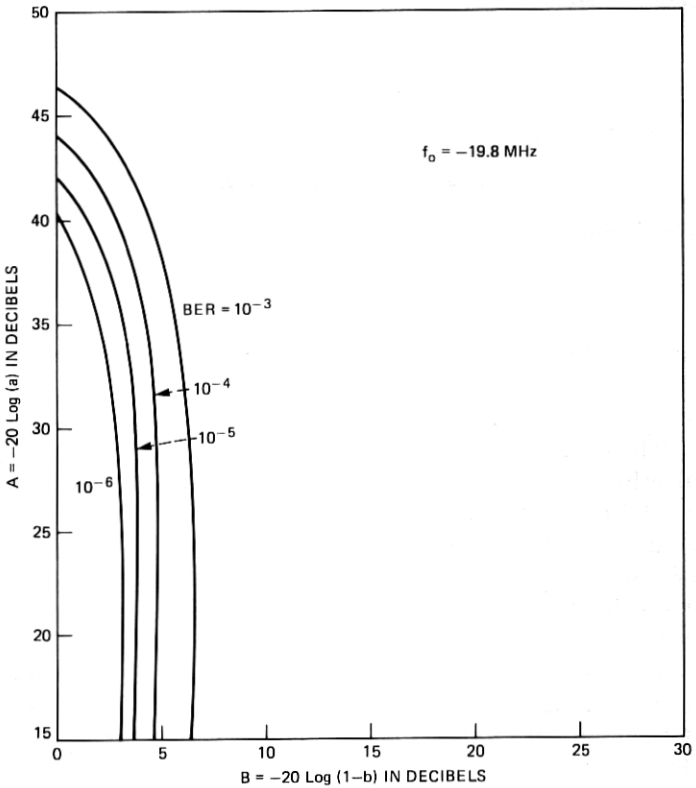

Fig. 10—Critical curves of A and B for $f_o = -19.8$ MHz.

$$P_o = \Delta\phi \sum_{\text{All } \phi_i} p_\phi(\phi_i) P_c(\phi_i). \tag{16}$$

To illustrate the calculation of outage probability with eqs. (15) and (16), we shall calculate the term in the summation of eq. (16) corresponding to a BER of 10^{-3} and $\phi_i = -45°$ (or $f_o = -19.8$ MHz). From Fig. 11, which is taken from Fig. 10, we note that the double integral in eq. (15) may be broken into integrations over two regions. Thus

$$P_c(\phi_i) = \int_{B_c}^{\infty} \int_{-\infty}^{\infty} p_A(Y) p_B(X)\, dY\, dX + \int_{0}^{B_c} \int_{A_c(X)}^{\infty} p_A(Y) p_B(X)\, dY\, dX, \tag{17}$$

where the two double integrals correspond to integrations over Regions 1 and 2, respectively, in Fig. 11. Outage due to the occurrence of A and B in Region 1 may be described as outage due only to shape or

selectivity. In Region 2, outage is due to the combined effects of signal loss and selectivity.

Using eqs. (5) and (6), the integral over Region 1 is obtained as $e^{-B_c/3.8}$. The contribution due to thermal noise and shape (Region 2) is slightly more complicated. Dividing the interval 0 to B_c in Fig. 11 into N subintervals, as shown in Fig. 12, the probability of being in Region 2 is the sum of the probabilities for each subinterval. Thus eq. (17) becomes

$$P_c(\phi_i) = e^{-B_c/3.8} + \sum_{k=1}^{N} [e^{-B_{k-1}/3.8} - e^{-B_k/3.8}] P_g\left(\frac{A_k - A_0(B_k)}{5}\right), \quad (18)$$

where

$$P_g(X) = \frac{1}{\sqrt{2\pi}} \int_X^\infty e^{-x^2/2}\, dx. \quad (19)$$

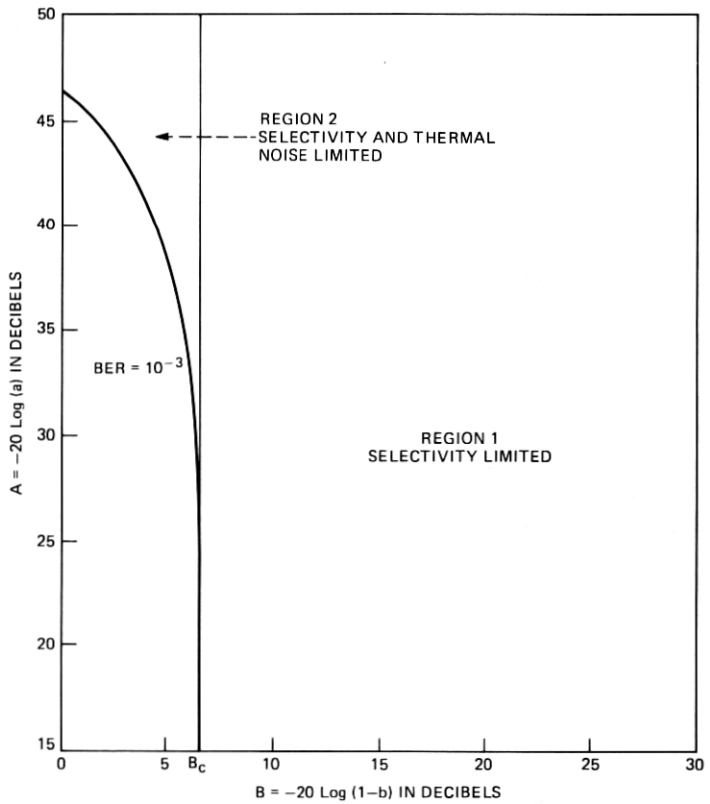

Fig. 11—Classification of outage with respect to critical curve for BER = 10^{-3}, f_0 = 19.8 MHz.

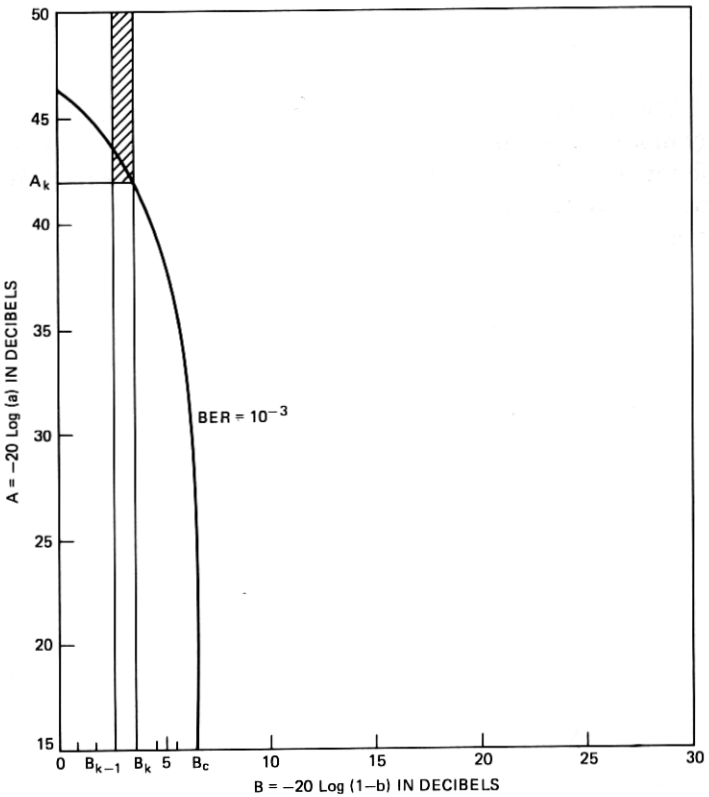

Fig. 12—Outage calculation for an incremental interval.

Evaluating the two components of eq. (18) from Fig. 11, we find

$$P_c(-45°) = 0.181 + 0.003 = 0.184. \tag{20}$$

This calculation was performed for 10 values of ϕ_i from −5 to −85 degrees in 10-degree steps. Using these results in eq. (16) and multiplying by two to account for positive values of ϕ_i which are assumed to contribute equally, we find the probability, P_o for a BER of 10^{-3} as

$$P_o = 0.0996.$$

The expected outage for the data base period is, then,

$$T_o = 5400 \times 0.0996 = 538 \text{ seconds}. \tag{21}$$

4.3 Outage calculation—selectivity only

It is apparent from eq. (20) that most of the outage for the system under study is caused by selectivity, fades characterized by A and B values in Region 1. From eqs. (14) and (17), we may express P_{os}, the probability of outage due to selectivity, as

$$P_{os} = \int_{-\pi}^{\pi} \int_{B_c}^{\infty} p_\phi(\phi) p_B(X)\, dX\, d\phi. \tag{22}$$

For the system studied for a BER of 10^{-3}, a finite B_c is obtained only for $|\phi_i| < 90$ degrees. Hence, we may use eq. (7) to simplify (22)*

$$P_{os} = \frac{2\Delta\phi}{216} \sum_{i=1}^{10} e^{-B_c(\phi_i)/3.8}. \tag{23}$$

From eq. (23) we see that the outage due only to selectivity depends on the relationship between B_c, the asymptote of critical B values, and the notch angle or notch frequency. Figure 13 shows the relationship between B_c and the notch frequency for four values of BER. It is apparent from eq. (22) that the outage probability is the probability of finding B and f_o values in the region above this curve. Such curves, therefore, provide a useful basis for evaluating the selectivity outage of a digital radio system.

4.4 Outage calculation— approximate method

For a radio system sensitive to both thermal noise and selectivity, the calculation of Section 4.3 is inadequate and that of Section 4.2 is unduly cumbersome.

To illustrate a simpler, but generally applicable, method and at the same time to provide a useful incidental result, let us evaluate the effect of reducing the transmitted power by 10 dB. For the reduced power system, the carrier-to-noise ratio would be 52 dB for the unfaded channel, and the critical curves of A and B would be shifted by 10 dB. Figure 14 shows the critical curve of A and B for a 10^{-3} BER and $f_o = -19.8$ MHz with an overplot of the conditional mean of the distribution of A. The dotted curves on Fig. 14 represent 2-sigma intervals on either side of the mean. From the properties of the Gaussian distribution, one may determine that more than 95 percent of the values of A and B will lie between these two dotted curves. We designate as A_m and B_m the coordinates of the intersection of two curves: the critical $A - B$ curve and the conditional mean curve. Then approximating the critical curve of A and B with a straight line segment tangent at (A_m, B_m), with slope s, we may approximate the probability of outage by integrating the probabilities over the region to the right of the tangent line. Using eqs. (15) and (16), we obtain

$$P_o = \Delta\phi \sum_{\text{All } \phi_i} p_\phi(\phi_i) \int_0^{\infty} \int_{A_m + s(B - B_m)}^{\infty} p_A(Y) p_B(X) dY\, dX. \tag{24}$$

---

* The factor of two is required in eq. (23) because the indicated summation corresponds to an integration only over negative notch frequencies ($\phi_i < 0$).

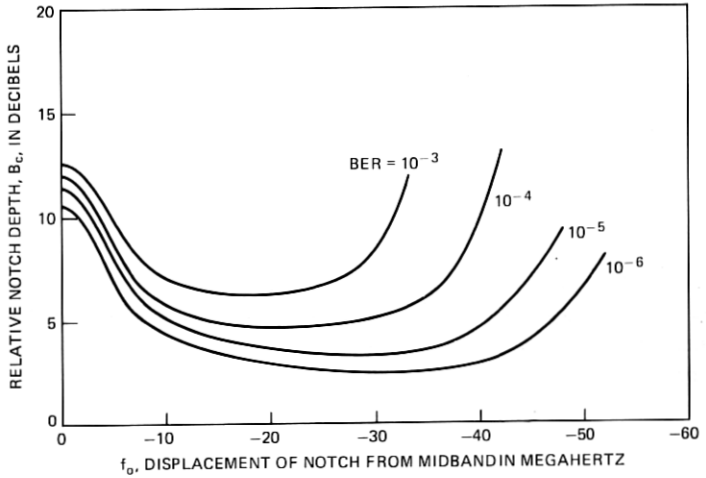

Fig. 13—Asymptotic performance curves. Locus of values of f_o and B that produce a fixed BER at high carrier-to-noise ratio.

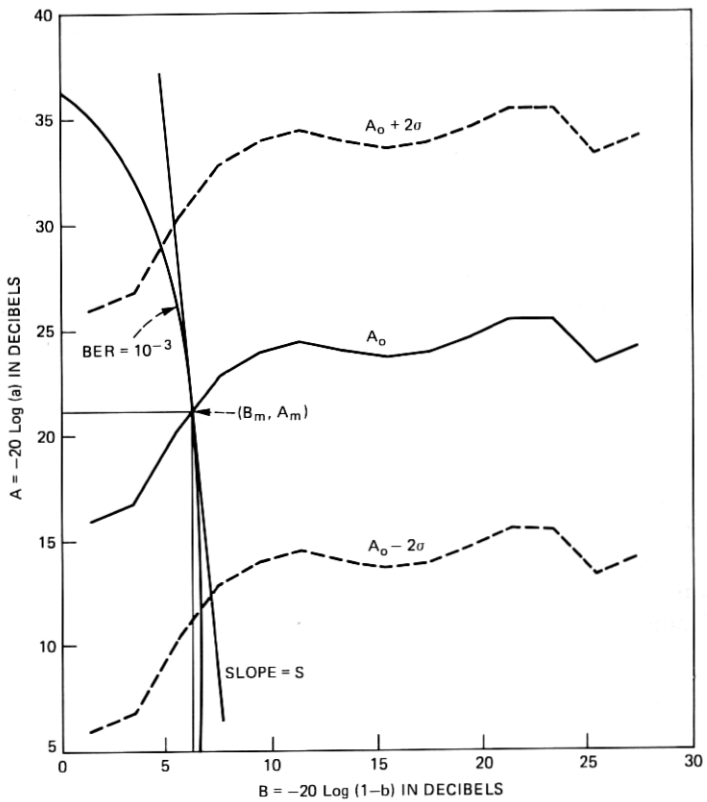

Fig. 14—Approximate outage calculation for 10 dB less transmitted signal.

Interchanging the order of integration and ignoring* the B dependence of $A_0(B)$, this becomes

$$P_o = \Delta\phi \sum_{\text{All } \phi_i} p_\phi(\phi_i) e^{-B_m/3.8} e^{0.866/s^2}. \tag{25}$$

Evaluating eq. (25) for a 10^{-3} BER and multiplying the result by 5400 gives an outage estimate for the data base period of 602 seconds. Recalculating the total outage time at a 10^{-3} BER using the method of Section 4.2 [eqs. (16) and (18)] gives 636 seconds, which verifies the accuracy of the approximate method. The estimate of 636 seconds was calculated as an upper bound; the 602 seconds calculated using (25) tend to be a lower bound. We conclude that backing off transmitted power by 10 dB would increase the outage by about 12 percent (538 to 602).

4.5 A further simplification

In this section, we show that the outage due to selectivity can be estimated approximately for a given BER from a determination of the in-band selectivity required (with the notch out-of-band) to produce that BER. Such a measurement may provide a useful approximation for any digital system using quadrature modulation components;[9] however, we provide a justification based on the performance of the system at hand. In-band selectivity is defined as the difference between the maximum and minimum attenuation present in the (25.3-MHz) channel bandwidth.

Since the in-band selectivity is a constant for any of the curves shown in Fig. 9, one can use Fig. 9 to plot the asymptotic BER against in-band selectivity for $f_o = -19.8$ MHz. Such a plot was generated for each notch position measured to produce the family of curves shown in Fig. 15. Note that, except for notch positions near the band center, the BER is uniquely related to the in-band selectivity. Neglecting the in-band notches, we find that a 10^{-3} BER corresponds to an in-band selectivity of 5.5 dB.

If we use the original model of eq. (2) to determine the values of B that will produce an in-band selectivity of 5.5 dB for a number of different notch positions, we would generate Fig. 16. It is apparent that for this system there is a good correspondence between the curves of asymptotic performance (Fig. 13) and the curves of constant in-band selectivity (Fig. 16).

To reinforce this conclusion, we provide Figs. 17, 18, and 19. Figure 17 shows the locus of in-band selectivity in a 25.3-MHz band corre-

* Including the effect of the slope of $A_0(B)$ at $B = B_m$ gives the same symbolic result with s interpreted as the algebraic sum of the slope of the tangent and dA_0/dB evaluated at $B = B_m$.

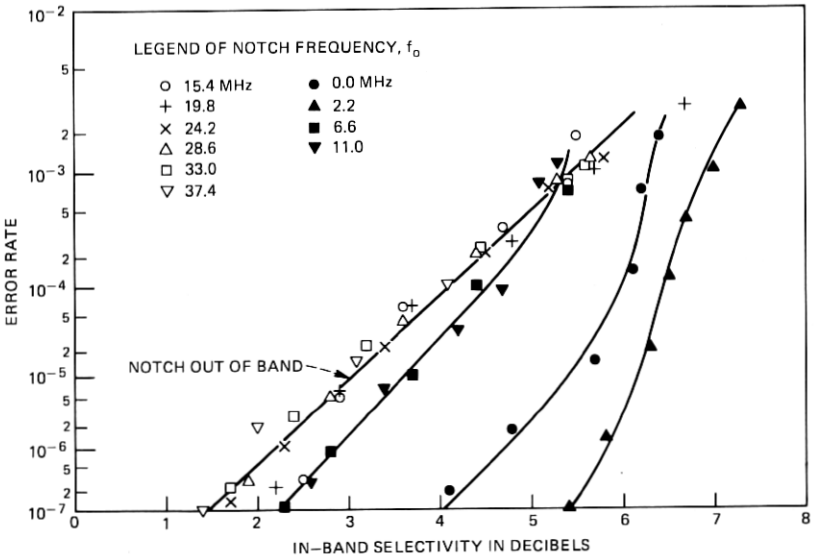

Fig. 15—Measured asymptotic bit error rate vs peak-to-peak amplitude difference in a 25.3-MHz band.

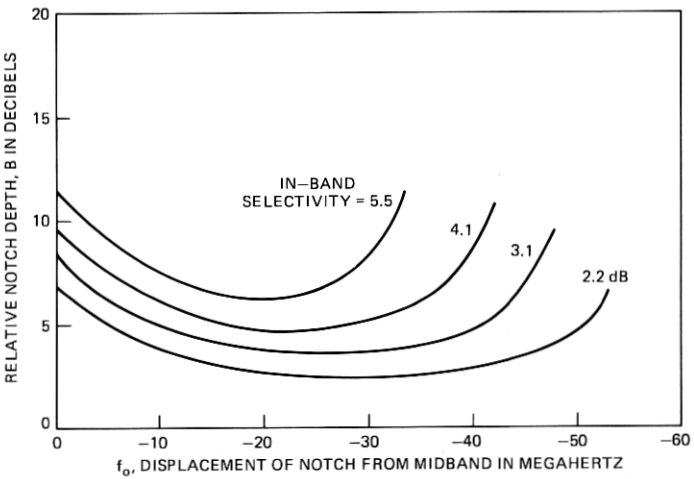

Fig. 16—Locus of B and f_o for modeled fades that have fixed peak-to-peak amplitude in a 25.3-MHz band.

sponding to each of the curves of constant BER in Fig. 13. That is, for each BER and each value of notch position, f_o, we have plotted the peak-to-peak amplitude difference in the band for the corresponding value of B_c, the asymptotic critical value of B. Figure 18 shows a similar set of curves with the peak-to-peak delay distortion in a 25.3-

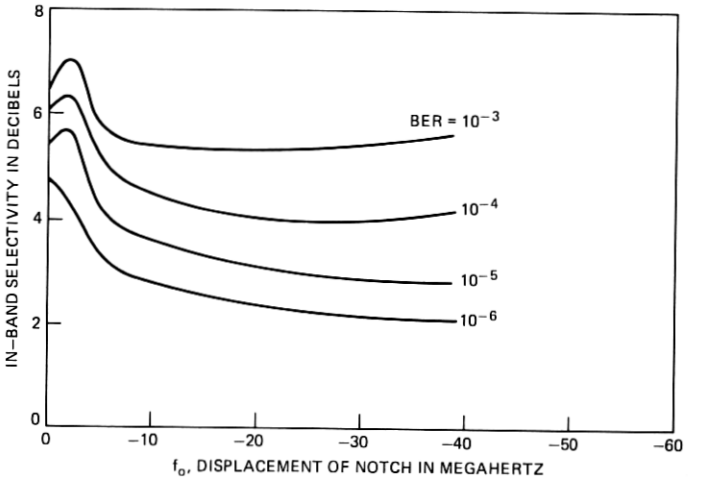

Fig. 17—In-band selectivity (in 25.3-MHz bandwidth) corresponding to asymptotic critical values of notch depth (B_c) for several values of BER.

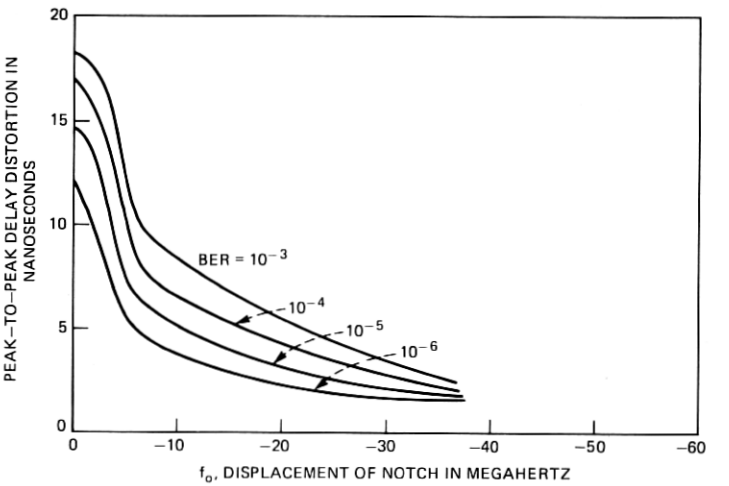

Fig. 18—Peak-to-peak envelope delay distortion in 25.3-MHz bandwidth corresponding to asymptotic critical values of notch depth (B_c) for several values of BER.

MHz band as the ordinate. Similarly, Fig. 19 has as the ordinate the "slope," or amplitude difference at a separation of 25.3 MHz. It is again clear from these three figures that the in-band selectivity is the relevant channel impairment giving rise to errors. We see from Fig. 18 that, for out-of-band notches, high BERs are obtained with very small values of peak-to-peak delay distortion, and from Fig. 19 that for in-band notches high BERs are obtained for very small values (zero at mid-band) of slope.

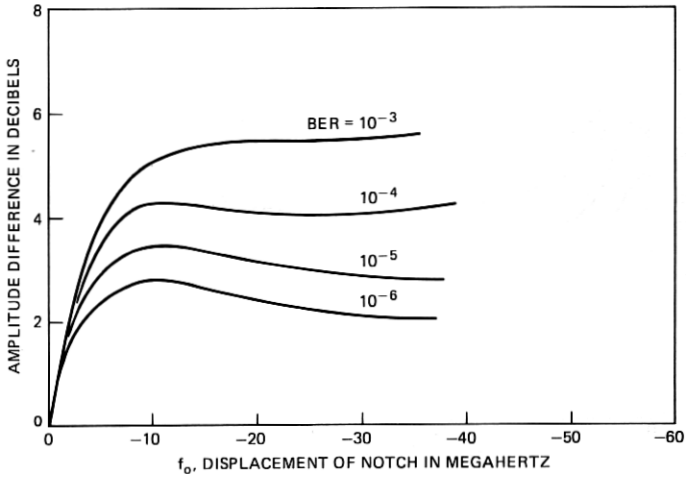

Fig. 19—Amplitude difference at a 25.3-MHz frequency separation corresponding to asymptotic critical values of notch depth (B_c) for several values of BER.

The model data base was analyzed to determine the time during which the in-band selectivity in a band of 25.3 MHz exceeded a given value. Figure 20 presents this distribution for in-band selectivity as calculated from the modeled fits. Figure 20 can be used directly in conjunction with Fig. 15 to calculate the outage times for the model data base.* For instance, from Fig. 15 we note that 5.5 dB of selectivity corresponds to a 10^{-3} BER. We use Fig. 20 to determine that 5.5 dB was exceeded for 520 seconds.

V. COMPARISONS OF CALCULATED AND OBSERVED OUTAGES

Using the methods of Sections 4.2 to 4.5, outage times were calculated for bit error rates of 10^{-3} to 10^{-6} for both the model data base period and for a heavy fading month, by multiplying the outage probabilities by 5400 and 8100, respectively.

5.1 Model data base period

Calculated and observed† outages for the model data base period are shown in Table I. In general, comparing the calculated results with observed results, we see that the outage is underestimated at high BERs and overestimated at low BERs. Any estimation procedure based on the current modeled state of the channel will tend to underestimate

* In practice, one would use a single measurement of in-band selectivity. For instance, in Fig. 9 one would take the 5.7-dB value corresponding to the curve asymptotic at a 10^{-3} BER.

† Because of quantization, the outage times observed from the field experiment correspond to bit error rates of 1.26×10^{-3}, 1.57×10^{-4}, 0.981×10^{-5}, and 1.19×10^{-6}.

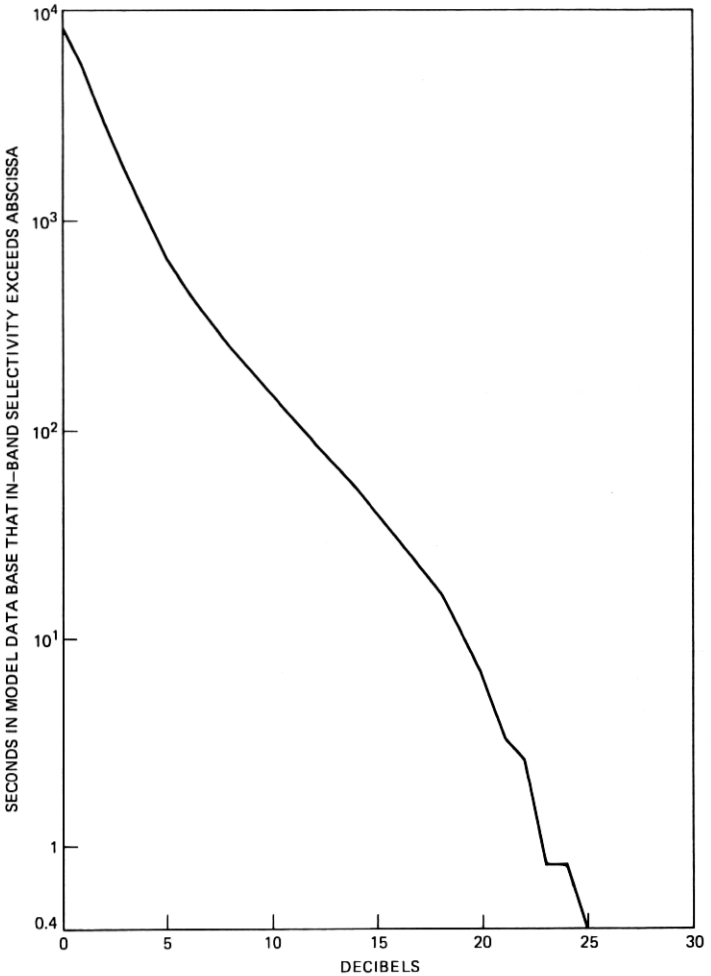

Fig. 20—Distribution of in-band selectivity (25.3-MHz bandwidth) for model data base.

Table I—Outage in modeling data base period (seconds)

BER =	10^{-3}	10^{-4}	10^{-5}	10^{-6}
Observed	636	903	1191	1487
Detailed calculation (Section 4.2)	538	960	1430	1860
Approximate calculation (Section 4.4)	527	950	1420	1830
Asymptotic calculation (Section 4.3)	527	950	1420	1830
Selectivity calculation (Section 4.5)	510	900	1570	2730

outage at high BERs because of hysteresis effects in the radio receiving equipment. That is, when the channel condition becomes sufficiently severe, the bit error rate becomes high enough (on the order of 10^{-3}) that the timing and/or phase of the radio system breaks lock. If the

channel impairment becomes less severe, the BER will not improve until the system resynchronizes. The hysteresis is important at the 10^{-3} BER, since a significant fraction of the events that cause 10^{-3} BER will cause the system to break lock.

One would expect to overestimate the outage at low BERs because of the method of taking data. Recall that, in measuring the curves in Fig. 9, it was found that the BER depended on the phase to which the system had locked. The recorded performance represented the worst-phase condition. At a 10^{-6} BER, the best phase produces a BER that is about ⅓ that produced by the worst phase; the difference in BER from worst to best phase at a 10^{-3} BER is negligible. Hence, one would expect outage to be overestimated significantly at low bit error rates.

In comparing the outage calculated from in-band selectivity (Section 4.5) to the outage observed, we find that the overestimation of outage at low BERs is more severe than with the other methods. This is due to the greater sensitivity of the differential selectivity method to the bias induced by choosing the worst-case phase. For instance, comparing calculations at a 10^{-6} BER, we find that Fig. 20 is steeper for amplitude differences near 2 dB than is Fig. 3 near B values of 3.5 dB. (Figure 9 verifies the appropriateness of this comparison). More generally, one expects the method based on in-band selectivity to overestimate the outage because the method is based on notches out of band. From Fig. 15, it is apparent that, for a given ΔA, some scans will not have the BER specified.

We conclude that, although calculation of outage from sensitivity to in-band selectivity provides quick estimates, they are less accurate. The calculation requires knowledge of the distribution of in-band selectivity over a specified bandwidth. These statistics are neither simple nor generally available. It has been shown,[10] for instance, that slope statistics have a nontrivial dependence upon the measurement bandwidth.

It is clear that the calculations based on selectivity (Sections 4.3 and 4.5) agree for the system studied here because that system has very little outage due to thermal noise limitations, and because it is sensitive primarily to in-band amplitude excursions. The extent to which these statements are true for other systems is currently unknown.

5.2 Outage on a monthly basis

The results in Table I may be put on the basis of a heavy fading month by increasing them by a factor of 1.5, as discussed in Section 2.2. The resulting outages (including the scaled observed outage) are compared with the outage observed in a one-month period[8] in Table II. We see that the outage times observed in the total one-month period agree well with the values obtained by scaling the observed

Table II—Outage in a heavy fading month (seconds)

BER =	10^{-3}	10^{-4}	10^{-5}	10^{-6}
Observed (Ref. 8)	1000	1320	2100	2900
Scaled observation from Table I	955	1350	1790	2230
Calculation (Section 4.2–4.4)	800	1430	2140	2760
Selectivity calculation (Section 4.5)	770	1350	2350	4100

outage for the data base period used in modeling, except for the slight divergence appearing at low BERs. This divergence should not be unexpected for this equipment. As may be seen in Fig. 15, a 10^{-6} BER may be caused by differential amplitude selectivity in band of 2 dB. Such modest amounts of selectivity may be expected to occur sometimes in the presence of very moderate selective fading. The modeling data base was constructed by selecting only periods of significant selective fading. This reinforces the comments made in conjunction with Fig. 3, namely, that the model distribution of B represents a lower bound for small values of B which can contribute to outage at the 10^{-6} BER level.

VI. CONCLUSIONS

We have demonstrated the validity of a technique for estimating the unprotected outage of a digital radio system due to selective fading on a particular hop in the 6-GHz common carrier band. The technique required field measurements to statistically characterize the parameters of a model of propagation on the hop. It also requires performance data obtained in the laboratory for the radio system by stressing it with a two-path fade simulator with a differential path delay of 6.3 ns, corresponding to the fixed delay channel model. Since the radio path on which these measurements were made has a length close to the average for the Bell System long haul radio network and has an average incidence of fading activity, the channel model is representative of a typical path. At the very least, the technique provides a basis for determining the relative merits of various digital radio systems operating without benefit of space diversity.

For the system under test, outage was calculated by four different methods. Because this system was selectivity-limited rather than noise-limited, all four methods predicted approximately the same outage as that summarized in Table I; however, the method based on in-band selectivity is more severely biased at low BERs. The method based on asymptotic performance and that based on in-band selectivity can only be used to estimate outage due to selectivity. If the transmitted power of the system under test were reduced by 10 dB, both of the other two methods, the detailed and the approximate method, would predict an increase in outage time of about 12 percent.

VII. ACKNOWLEDGMENTS

The conclusions of this effort depend upon data collected on a 6-GHz digital radio hop installed by R. A. Hohmann and L. J. Morris, using instrumentation designed by G. A. Zimmerman. M. V. Pursley's assistance in processing the data was invaluable. Consistent laboratory data used to close the loop reflect contributions by T. J. West and G. B. Thomas to the methodology of selective fade simulation at IF, and A. E. Resch who performed the measurements.

REFERENCES

1. E. Takeuchi and P. Tobey, "A 6 GHz Radio for Telephony Applications," Conference Record ICC 1976, Vol. II, June 1976, p. 18–27.
2. P. R. Hartman and J. A. Crossett, "A 90 MBS Digital Transmission System at 11 GHz using 8 PSK Modulation," Conference Record ICC 1976, Vol. II, June 1976, p. 18–8.
3. A. J. Giger and T. L. Osborne, "3A-RDS 11 GHz Digital Radio System," Conference Record ICC 1976, Vol. II, June 1976, p. 18–1.
4. I. Godier, "DRS-8 Digital Radio for Long-Haul Transmission," Convention Record ICC 1977, Vol. 1, June 1977, p. 102.
5. W. A. H. Wood, "Modulation and Filtering Techniques for 3 Bits/Hertz Operation in the 6 GHz Frequency Band," Convention Record ICC 1977, Vol I, June 1977, p. 97.
6. W. D. Rummler, "A New Selective Fading Model: Application to Propagation Data," B.S.T.J, this issue, pp. 1037–1071.
7. W. T. Barnett, "Multipath Propagation at 4, 6, and 11 GHz," B.S.T.J., *51*, No. 2 (February 1972), pp. 321–361.
8. W. T. Barnett, "Measured Performance of a High Capacity 6 GHz Digital Radio System," Conference Record ICC 1978, Vol. III, June 1978, pp 47.4.1–47.4.6.
9. J. R. Gray and T. J. West, private communication.
10. G. M. Babler, "A Study of Frequency Selective Fading for a Microwave Line-of-Sight Narrowband Radio Channel," B.S.T.J., *51*, No. 3 (March 1972), pp. 731–757.